**Supplemental Materials**

Supplemental Figure Legends:

**Figure S1. Molecular Phylogenetic analysis of VC20013 *envelope* sequences by Maximum Likelihood method.** The evolutionary history of the *envelope* sequences from subject VC20013 was inferred by using the Maximum Likelihood method based on the Tamura-Nei model (6). The tree with the highest log likelihood (-8131.4010) is shown. The percentage of trees in which the associated taxa clustered together is shown next to the branches. Initial tree(s) for the heuristic search were obtained automatically by applying Neighbor-Join and BioNJ algorithms to a matrix of pairwise distances estimated using the Maximum Composite Likelihood (MCL) approach, and then selecting the topology with superior log likelihood value. The tree is drawn to scale, with branch lengths measured in the number of substitutions per site. The analysis involved 56 nucleotide sequences. All positions containing gaps and missing data were eliminated. There were a total of 2386 positions in the final dataset. Evolutionary analyses were conducted in MEGA6 (7).

**Figure S2. Molecular Phylogenetic analysis of VC10014 *envelope* sequences by Maximum Likelihood method.** The evolutionary history of the *envelope* sequences from subject VC10014 was inferred by using the Maximum Likelihood method based on the Tamura-Nei model, as in Figure S1 (6). The tree with the highest log likelihood (-8318.4416) is shown. The analysis involved 51 nucleotide sequences. There were a total of 2497 positions in the final dataset. Evolutionary analyses were conducted in MEGA6 (7).

**Figure S3. Analysis of glycan-specific bNAb epitope activity in the heterologous virus SC422661.8.** To test for glycan specific bNAb activity in the plasma of VC20013, we used a combination of pseudo-viruses grown in glycosidase inhibitors (A) and point mutation knock outs of N-linked glycosylation sites (B). A) SC422661.8 pseudo-virus was grown in 293T cells in the absence of glycosidase inhibitors, in the presence of swainsonine, and in the presence of kifunensine, and all three stocks were normalized for viral entry before use in the neutralization assay. The pseudo-viruses were tested against VC20013 plasma from 2.76 years post infection, which was titrated from 1:20 – 1:14580. B) N-Q point mutations were introduced into SC422661.8 at N-linked glycosylation sites known to be critical for binding to bNAbs PG9/PG16 (9), 2G12 (5), and PGT128 (8). The N-Q point mutation disrupts the N-X-S/T glycosylation motif, preventing the attachment of glycan residues. Plasma from VC20013 from 2.76 years post infection was titrated 1:20-1:14580.

**Figure S4. Sequence identity in the membrane proximal external region of the autologous VC20013 *envelopes***. The MPER region of the autologous *envelopes* were aligned using the MUSCLE alignment algorithm (1, 2). The sequence logo at the top of the figure is representative of the proportion of sequences that harbor a given amino acid residue. The horizontal line denotes the separation between the time points with and without bNAb activity in the plasma. The MPER residue at position 677, which we determined was an escape mutation from the bNAb activity in VC20013, is surrounded by a red box.

**Figure S5. Analysis of glycan-specific bNAb epitope activity in the heterologous virus SC422661.8.** To test for glycan specific bNAb activity in the plasma of VC10014, we used a combination of SC422661.8 pseudo-viruses grown in glycosidase inhibitors (A) and point mutation knock outs of N-linked glycosylation sites (B), as in Figure S1. A) Neutralization of glycosidase inhibitor-grown SC422661.8 pseudovirus by VC10014 plasma from 3.59 years post infection. B) Neutralization of NLGS-mutated pseudovirus by VC10014 plasma from 3.59 years post infection.

**Figure S6. Neutralization of VC10014 autologous isolates by gp120 and gp120$_{D368R}$-depleted plasma.** Plasma from 6 years post infection was fractionated on gp120 and gp120$_{D368R}$ coated magnetic beads and tested against autologous pseudo-virus, as previously reported (3, 4). The un-depleted, gp120-depleted, and gp120$_{D368R}$ depleted (which leaves anti-CD4-BS antibodies intact in the plasma) fractions were tested against autologous pseudo-virus from A) 1.3 years post infection and B) 3.22 years post infection. The horizontal red lines indicate the IC50, which is the dilution of plasma at which neutralization was reduced to 50%, and the vertical red lines denote the approximate IC50 dilution value for each sample. The shift to the left in the vertical red line from the un-depleted plasma (light blue circles) to gp120-depleted plasma (green triangles) or gp120$_{D368R}$ depleted plasma indicates a reduction in neutralization potential of the depleted plasma.

**Figure S7. Sequence alignments of the C2 and V4 regions in the autologous VC10014 *envelopes***. The C2 (A) and V4 (B) regions of the autologous *envelopes* were aligned using the MUSCLE alignment algorithm (1, 2). The sequence logo at the top of the figure is representative of the proportion of sequences that harbor a given amino acid residue. The horizontal line denotes the separation between the time points with and without bNAb activity in the plasma. A) The potential escape mutations in residues 277 and 279 in the C2 are enclosed in the red box. B) The potential escape mutations in the V4, in which four amino acids were inserted into the V4 loop, are enclosed by a red box.

Figure S1.

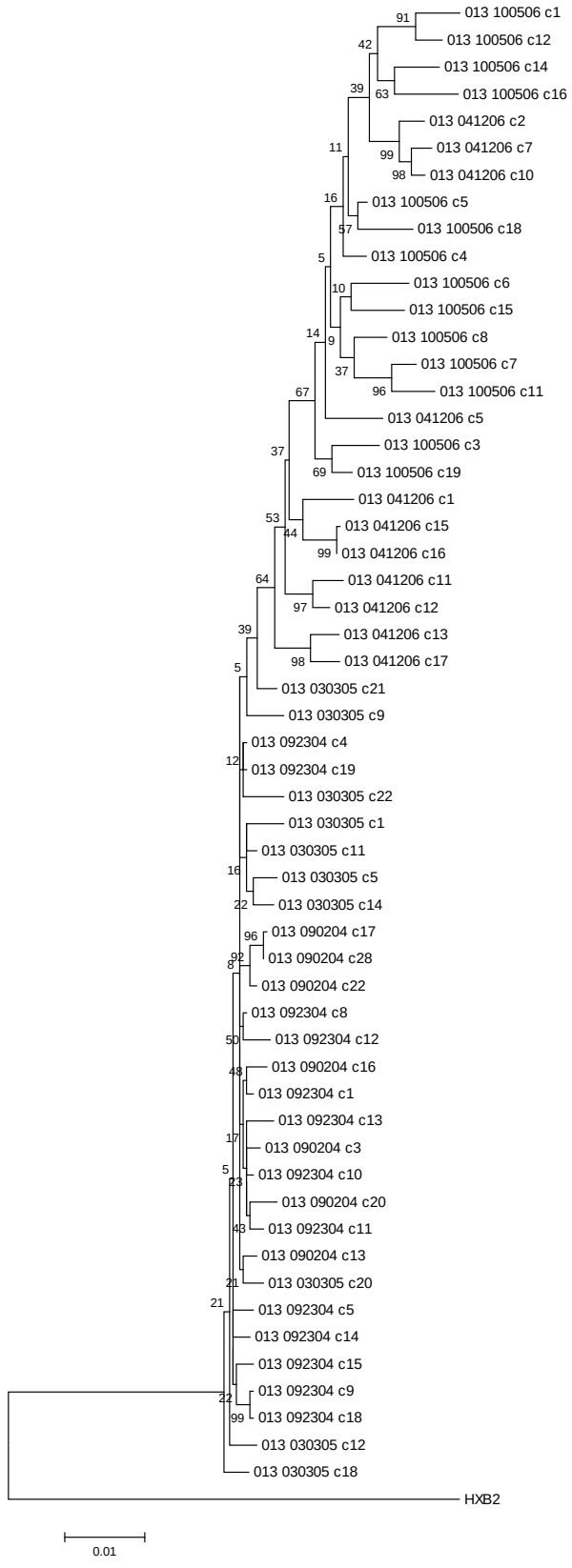
013 100506 c1
013 100506 c12
013 100506 c14
013 100506 c16
013 041206 c2
013 041206 c7
013 041206 c10
013 100506 c5
013 100506 c18
013 100506 c4
013 100506 c6
013 100506 c15
013 100506 c8
013 100506 c7
013 100506 c11
013 041206 c5
013 100506 c3
013 100506 c19
013 041206 c1
013 041206 c15
013 041206 c16
013 041206 c11
013 041206 c12
013 041206 c13
013 041206 c17
013 030305 c21
013 030305 c9
013 092304 c4
013 092304 c19
013 030305 c22
013 030305 c1
013 030305 c11
013 030305 c5
013 030305 c14
013 090204 c17
013 090204 c28
013 090204 c22
013 092304 c8
013 092304 c12
013 090204 c16
013 092304 c1
013 092304 c13
013 090204 c3
013 092304 c10
013 090204 c20
013 092304 c11
013 090204 c13
013 030305 c20
013 092304 c5
013 092304 c14
013 092304 c15
013 092304 c9
013 092304 c18
013 030305 c12
013 030305 c18
HXB2
0.01

**Figure S2.**

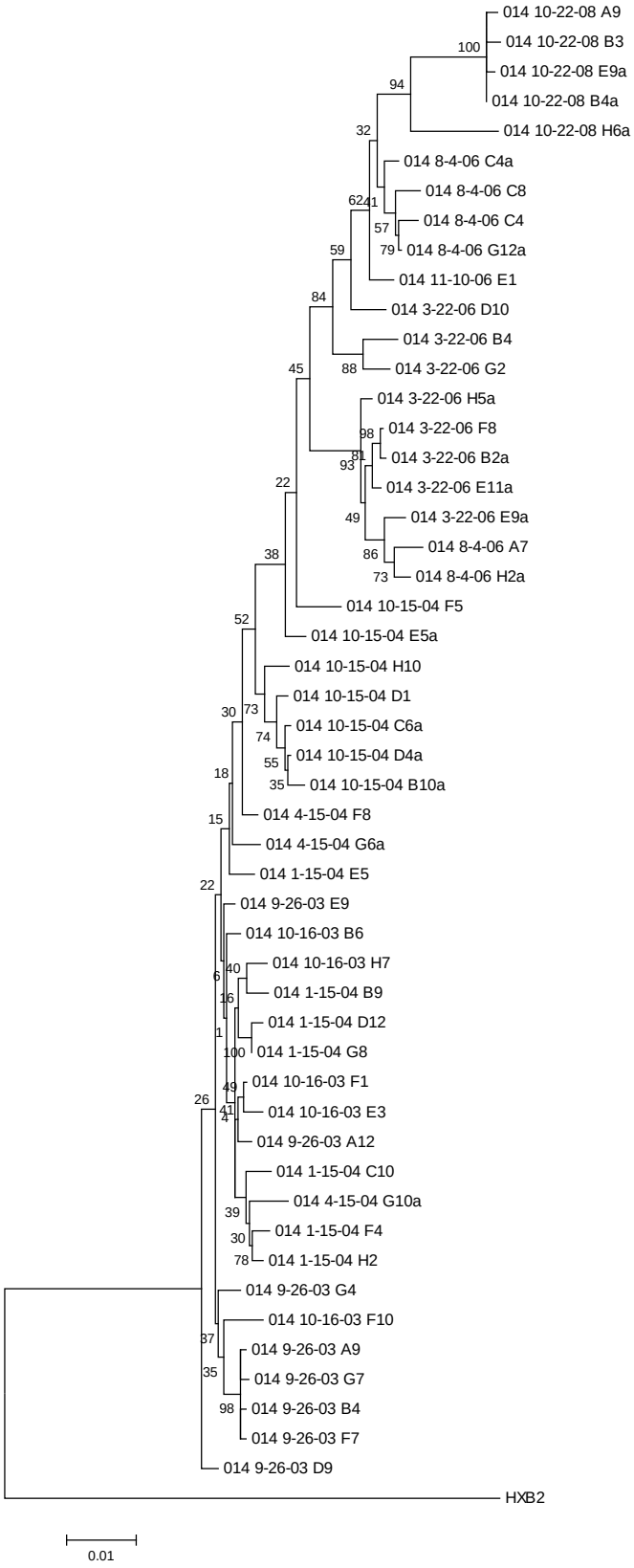
014 10-22-08 A9
014 10-22-08 B3
014 10-22-08 E9a
014 10-22-08 B4a
014 10-22-08 H6a
014 8-4-06 C4a
014 8-4-06 C8
014 8-4-06 C4
014 8-4-06 G12a
014 11-10-06 E1
014 3-22-06 D10
014 3-22-06 B4
014 3-22-06 G2
014 3-22-06 H5a
014 3-22-06 F8
014 3-22-06 B2a
014 3-22-06 E11a
014 3-22-06 E9a
014 8-4-06 A7
014 8-4-06 H2a
014 10-15-04 F5
014 10-15-04 E5a
014 10-15-04 H10
014 10-15-04 D1
014 10-15-04 C6a
014 10-15-04 D4a
014 10-15-04 B10a
014 4-15-04 F8
014 4-15-04 G6a
014 1-15-04 E5
014 9-26-03 E9
014 10-16-03 B6
014 10-16-03 H7
014 1-15-04 B9
014 1-15-04 D12
014 1-15-04 G8
014 10-16-03 F1
014 10-16-03 E3
014 9-26-03 A12
014 1-15-04 C10
014 4-15-04 G10a
014 1-15-04 F4
014 1-15-04 H2
014 9-26-03 G4
014 10-16-03 F10
014 9-26-03 A9
014 9-26-03 G7
014 9-26-03 B4
014 9-26-03 F7
014 9-26-03 D9
HXB2
0.01

**Figure S3**

A.

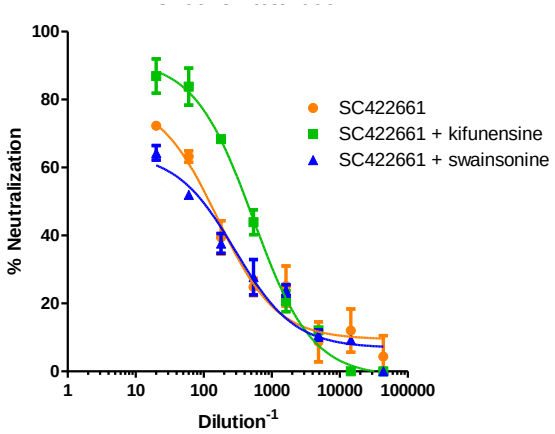
100
80
60
40
20
0
% Neutralization
1
10
100
1000
10000
100000
Dilution-1
SC422661
SC422661 + kifunensine
SC422661 + swainsonine

B.

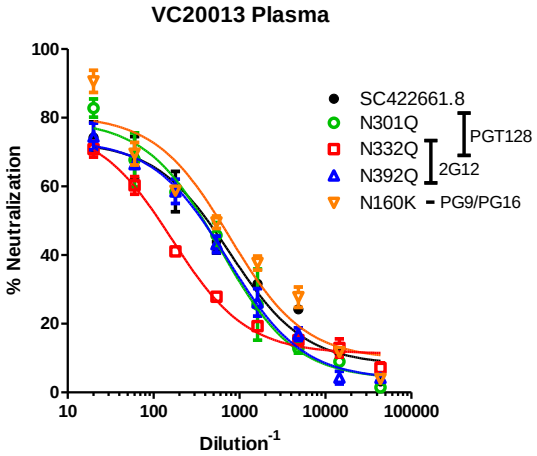
VC20013 Plasma
100
80
60
40
20
0
% Neutralization
10
100
1000
10000
100000
Dilution-1
SC422661.8
N301Q
N332Q
N392Q
N160K
PGT128
2G12
PG9/PG16

**Figure S4**

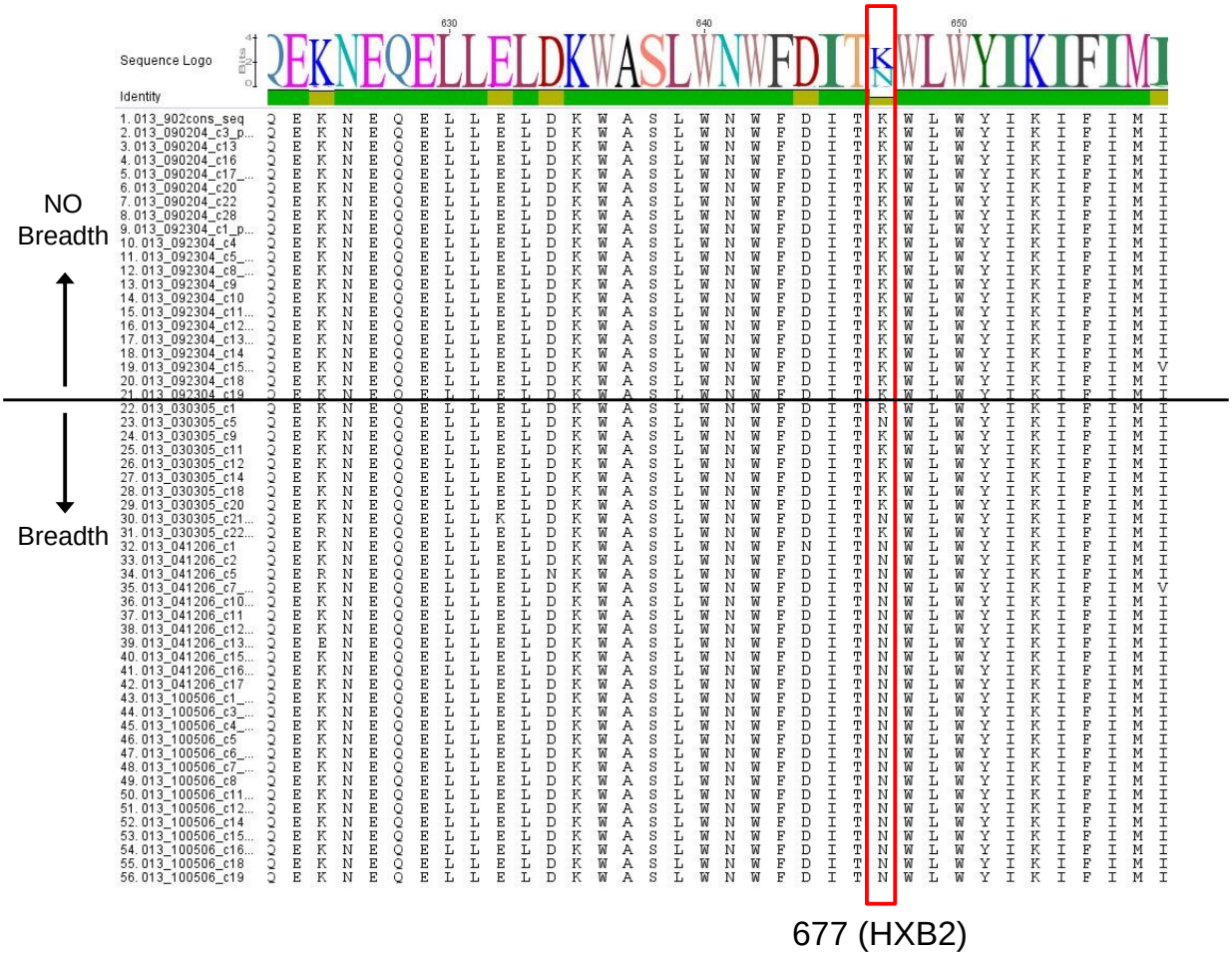
Sequence Logo
Identity
630
640
650
NO Breadth
Breadth
677 (HXB2)

**Figure S5**

A.

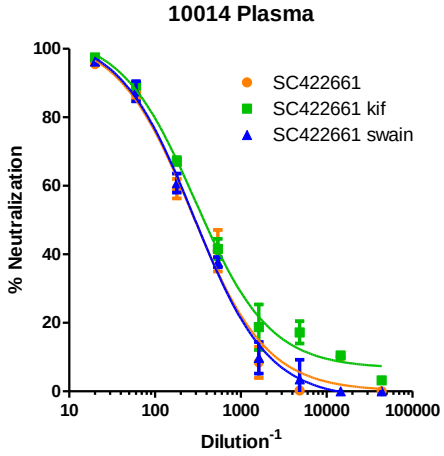
10014 Plasma
% Neutralization
Dilution-1
SC422661
SC422661 kif
SC422661 swain

B.

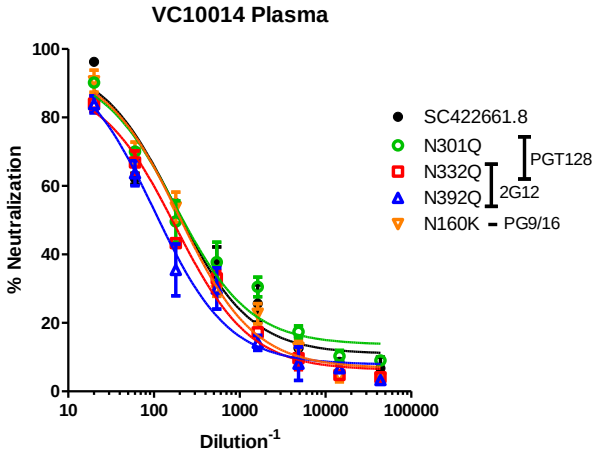
VC10014 Plasma
% Neutralization
Dilution-1
SC422661.8
N301Q
N332Q
N392Q
N160K
PGT128
2G12
PG9/16

**Figure S6**

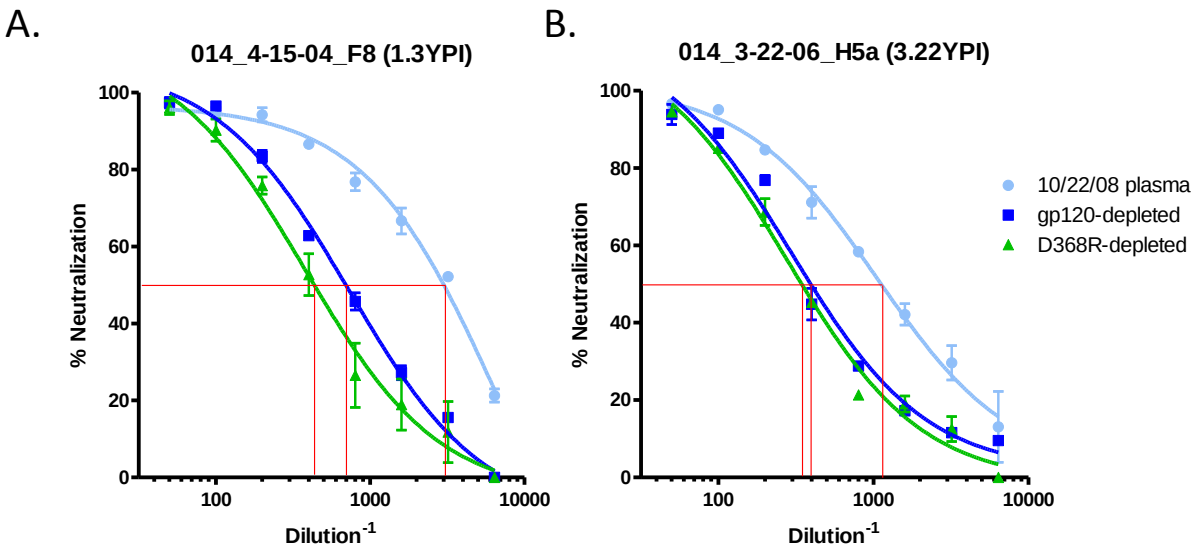
A.
014_4-15-04_F8 (1.3YPI)
% Neutralization
100
80
60
40
20
0
100
1000
10000
Dilution-1
B.
014_3-22-06_H5a (3.22YPI)
% Neutralization
100
80
60
40
20
0
100
1000
10000
Dilution-1
10/22/08 plasma
gp120-depleted
D368R-depleted

**Figure S7**

A.

C2 region

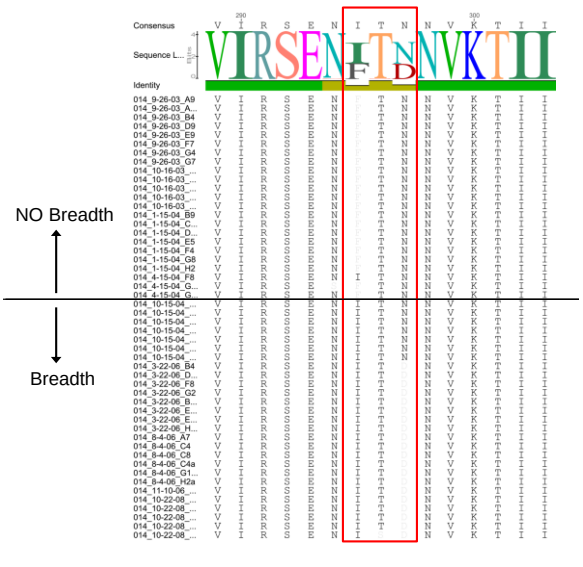


B.

V4 region

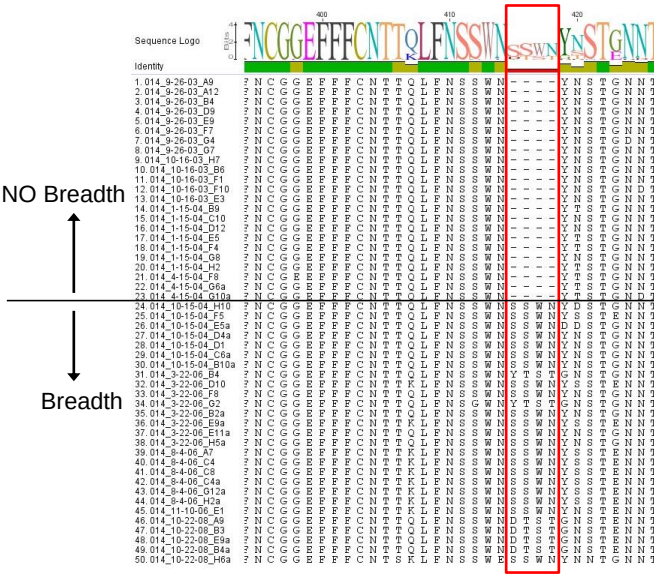

## References


1. **Edgar, R. C.** 2004. MUSCLE: a multiple sequence alignment method with reduced time and space complexity. BMC Bioinformatics **5:**113.
2. **Edgar, R. C.** 2004. MUSCLE: multiple sequence alignment with high accuracy and high throughput. Nucleic Acids Res **32:**1792-1797.
3. **Li, Y., S. A. Migueles, B. Welcher, K. Svehla, A. Phogat, M. K. Louder, X. Wu, G. M. Shaw, M. Connors, R. T. Wyatt, and J. R. Mascola.** 2007. Broad HIV-1 neutralization mediated by CD4-binding site antibodies. Nature medicine **13:**1032-1034.
4. **Sather, D. N., J. Armann, L. K. Ching, A. Mavrantoni, G. Sellhorn, Z. Caldwell, X. Yu, B. Wood, S. Self, S. Kalams, and L. Stamatatos.** 2009. Factors associated with the development of cross-reactive neutralizing antibodies during human immunodeficiency virus type 1 infection. J Virol **83:**757-769.
5. **Scanlan, C. N., R. Pantophlet, M. R. Wormald, E. Ollmann Saphire, R. Stanfield, I. A. Wilson, H. Katinger, R. A. Dwek, P. M. Rudd, and D. R. Burton.** 2002. The broadly neutralizing anti-human immunodeficiency virus type 1 antibody 2G12 recognizes a cluster of alpha1-->2 mannose residues on the outer face of gp120. J Virol **76:**7306-7321.
6. **Tamura, K., and M. Nei.** 1993. Estimation of the number of nucleotide substitutions in the control region of mitochondrial DNA in humans and chimpanzees. Mol Biol Evol **10:**512-526.
7. **Tamura, K., G. Stecher, D. Peterson, A. Filipski, and S. Kumar.** 2013. MEGA6: Molecular Evolutionary Genetics Analysis version 6.0. Mol Biol Evol **30:**2725-2729.
8. **Walker, L. M., M. Huber, K. J. Doores, E. Falkowska, R. Pejchal, J. P. Julien, S. K. Wang, A. Ramos, P. Y. Chan-Hui, M. Moyle, J. L. Mitcham, P. W. Hammond, O. A. Olsen, P. Phung, S. Fling, C. H. Wong, S. Phogat, T. Wrin, M. D. Simek, G. P. I. Protocol, W. C. Koff, I. A. Wilson, D. R. Burton, and P. Poignard.** 2011. Broad neutralization coverage of HIV by multiple highly potent antibodies. Nature **477:**466-470.
9. **Walker, L. M., S. K. Phogat, P. Y. Chan-Hui, D. Wagner, P. Phung, J. L. Goss, T. Wrin, M. D. Simek, S. Fling, J. L. Mitcham, J. K. Lehrman, F. H. Priddy, O. A. Olsen, S. M. Frey, P. W. Hammond, G. P. I. Protocol, S. Kaminsky, T. Zamb, M. Moyle, W. C. Koff, P. Poignard, and D. R. Burton.** 2009. Broad and potent neutralizing antibodies from an African donor reveal a new HIV-1 vaccine target. Science (New York, N.Y **326:**285-289.